The Effect of Interfacial Properties on Damage Evolution in Model Composites

Thomas J. Mackin, Teresa L. Halverson
Department of Mechanical and Industrial Engineering, The University of Illinois at Urbana-Champaign, 1206 W. Green St., Urbana, Illinois 61801

Nancy R. Sottos
Department of Theoretical and Applied Mechanics, The University of Illinois at Urbana-Champaign, 1206 W. Green St., Urbana, Illinois 61801

This study explores the effect of interfacial properties on damage evolution and damage mechanisms in model glass fiber reinforced epoxy matrix composites. The composite properties were varied by changing the interfacial bond between the fiber and the matrix. Double-edge-notched specimens were tested in tension and evaluated using thermoelastic stress analysis (TSA) to observe damage initiation and evolution, and to identify the operative damage mechanism. Changing the interface properties was found to change the operative damage mechanism. This study conclusively demonstrates that the damage mechanism in composites can be controlled by judicious changes in the interface properties.
POLYM. COMPOS., 26:241–246, 2005.

INTRODUCTION

Continued improvements in thrust-to-weight ratios of aircraft depend upon the development of new materials that are lighter, stiffer, and stronger at elevated temperatures. In order to implement new composites, it is important to understand how stress concentrations, such as holes, notches, lap joints, and incidental damage, will affect the residual strength and lifetime of the proposed composite systems. Furthermore, design guidelines must be developed to facilitate the safe and effective use of new materials. Regardless of the material used, damage tolerance is a crucial factor in design and plays a key role in establishing factors of safety. The current research aims to address the issue of damage tolerance by investigating two key questions: First, is it possible to control the damage mechanism by changing the interface properties? Second, how does the damage mechanism affect damage tolerance and stress redistribution in the composite?

Fiber reinforced composites redistribute stress around local sites of strain concentration through a combination of damage mechanisms, including: fiber failure and pullout, matrix cracking, interface debonding, and shear band development [1–6]. Several key damage mechanisms have been identified in composites, including:

(i) The propagation of a single matrix crack accompanied by fiber fracture and pullout (Class I);
(ii) The formation of multiple matrix cracks in the absence of fiber failure (Class II);
(iii) The formation of shear bands parallel to the loading axis (Class III) [3].

In any composite, combinations of these damage mechanisms may exist [1, 5–10].

It is well known that the structure and properties of the fiber/matrix interface affect the overall mechanical properties of all types of composites [11–23]. In particular, the durability characteristics such as strength and fracture toughness are strongly dependent upon the interfacial properties: a strong bond between fiber and matrix facilitates efficient load transfer between the constituents, while a weak interface promotes composite toughness by deflecting cracks into the fiber/matrix interface. The change in toughness is brought about by a change in micro-mechanisms. Studies of energy dissipation at the interface have shown that the toughening contribution from frictional sliding of the fiber is much greater than that of fiber debonding [18–23]. Bao and Suo [7] showed that mode I fracture toughness for a composite is explicitly dependent upon the size of the fiber bridging zone. The bridging zone length was in turn shown to be dependent on not only the fiber strength but also the fiber–matrix interface's capacity to transfer shear stress before and after debonding.

Correspondence to: T.J. Mackin; e-mail: tmackin@uiuc.edu
DOI 10.1002/pc.20065
Published online in Wiley InterScience (www.interscience.wiley.com).

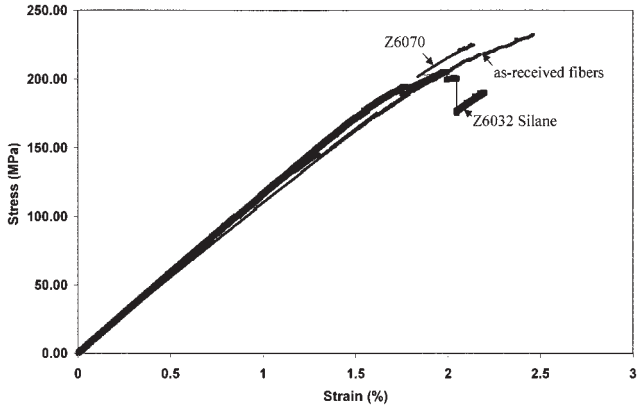

FIG. 1. Typical stress-strain curves for 636 glass/epoxy composites with $V_f \cong 12\%$.

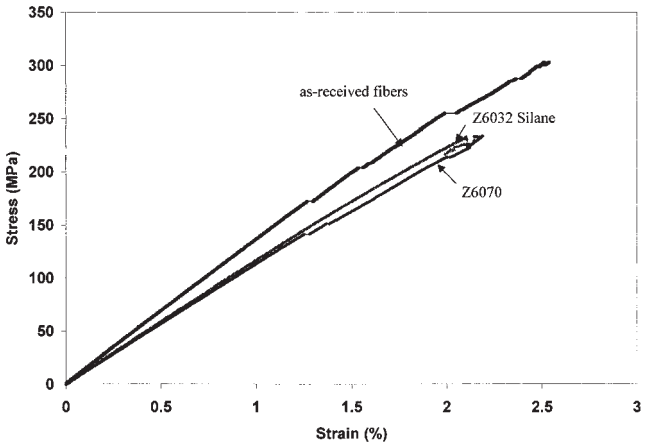

FIG. 2. Typical stress-strain curves for 646 glass/epoxy composites with $V_f \cong 12\%$.

Damage accumulation in the region of the interface is responsible for pseudo-ductility in composite materials, which is a key to stress redistribution. Understanding how the interfacial properties are correlated with the damage modes and size of the bridging zone is crucial for designing a composite for a desired application. For a given damage mechanism, any changes in constituent properties that improve the composite ductility will improve composite damage tolerance. The role of constituent characteristics on composite damage evolution and failure mechanisms has only recently emerged as an important area of study [2, 10–15]. The present study aims to add to that developing body of knowledge by investigating the affects of the interphase on damage evolution in model composites.

EXPERIMENTAL

Model Composites

Model composites consisting of unidirectional glass fibers in an epoxy matrix were utilized to study the effect of composite constituent properties on damage evolution in brittle matrix composites. The fiber volume fraction, the fiber/matrix interface, and the fiber strength distribution were altered in the glass/epoxy system. Fiber volume fractions ranged from 6% to 12% in the model composites. Though these are low volume fractions, they were sufficient to illustrate the affect of interface treatments on the operative damage mechanism.

Commercial E-glass fiber bundles with two different as-received surface treatments were obtained from Owens-Corning: 636 glass fiber utilizes an industry-standard starch coating that aids in winding, while 646 glass fibers have a coating composed of starch plus an added silane that helps protect the fibers from moisture damage. Each bundle consisted of 204 individual G150 type filaments with a nominal diameter of nine microns. Due to the presence of the silane surface treatment, the 646 fibers have a strength advantage over the 636 fibers [24]. The interface properties in the model systems were also modified by adding commercially available silanes to the matrix. Dow Corning® coupling agent Z6032 (aminoproply-trimethoxysilane) and dispersion agent Z6070 (methyl-trimethoxysilane) were utilized to enhance or weaken the interface bond, respectively.

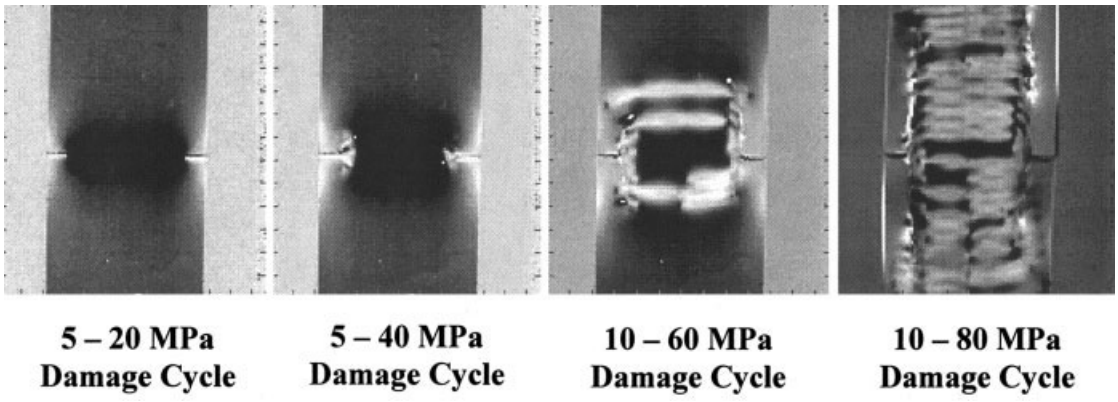

FIG. 3. Sequence of TSA images shows that damage evolves as multiple matrix cracks in the 636 glass/epoxy composite with as-received fibers, $V_f \cong 12\%$, and a/W = 0.25.

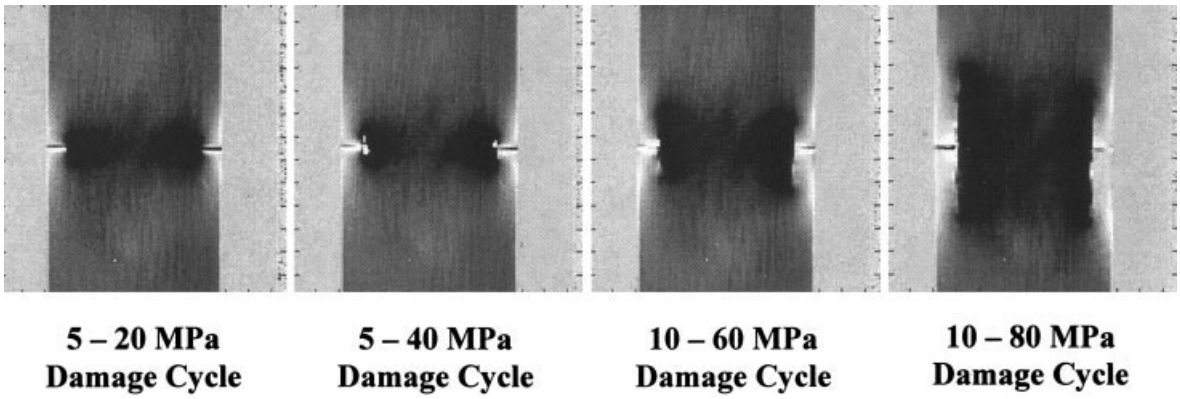

FIG. 4. Sequence of TSA images shows that damage evolves as shear bands in the 646 glass/epoxy composite with as-received fibers, $V_f \cong 12\%$, and a/W = 0.25.

Sample Preparation

Unidirectional glass fiber reinforced epoxy specimens were fabricated using a mini-filament winder. A counter was attached to the winder to provide a precise record of the absolute number of fibers in each composite. Fibers were dry-wound over silicone rubber molds that were fabricated according to ASTM standards. However, the ASTM standard shape (D3039/D3039M-95a) [25] was slightly modified by narrowing the width of the gage section and shouldering the grip sections in order to prevent grip failures during testing. Epoxy was poured into the molds following filament winding. The epoxy matrix was prepared by thoroughly mixing EPON 828 (diglycidyl ether of bisphenol A) resin with 12% by weight of diethylene-triamine (DETA) curing agent. For those samples with a modified interface bond, 1% by weight of coupling agent (Z6032) or dispersion agent (Z6070) was added to the epoxy resin before pouring. Finally, the entire mold was degassed in a vacuum chamber to minimize the amount of entrained air between the fibers. The specimens were then cured at room temperature for four days.

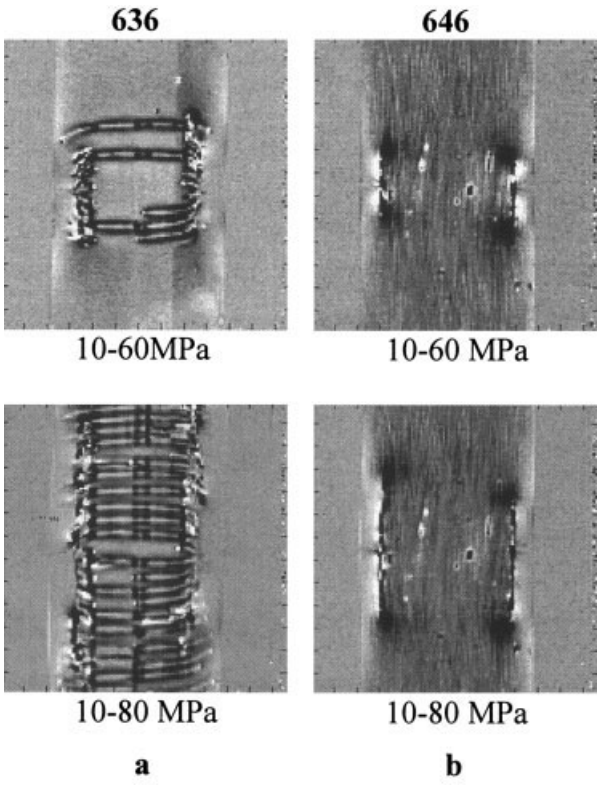

FIG. 5. Out-of-phase damage images clearly indicate that damage appears as multiple matrix cracks in the 636-glass/epoxy (a) and shear bands in the 646-glass/epoxy (b).

Before testing, the specimen surfaces were milled flat, sample dimensions were recorded, and the fiber volume fraction was calculated. The grip sections of all samples were tabbed with sections cut from fiberglass PC board in order to dissipate gripping stresses and prevent crushing of the sample end-sections in the tensile grips. Specimens for thermoelastic stress analysis were double-edge notched using a diamond blade at two different notch-to-width ratios: a/W = 0.125 and a/W = 0.25.

Experimental Method

Un-notched specimens were tested in tension at a crosshead rate of 0.03 mm/sec using an Instron 8500 with a 100 kN load cell (Figs. 1 and 2). Photographs were taken during each test to create a record of damage sequenced to the stress-strain response. The un-notched tensile curves were utilized to determine a loading schedule for damage evolution testing.

Thermoelastic stress analysis was used to map stress redistribution as a result of damage evolution in the composites during loading.[1] TSA relates instantaneous changes in the stress-state to instantaneous changes in the temperature. In the TSA method, a sinusoidal load is applied to the specimen that generates a cyclic temperature change that is in-phase with the applied load, according to:

[1] Delta Therm 1000 TSA system. Stress Photonics, Inc. Madison, WI.

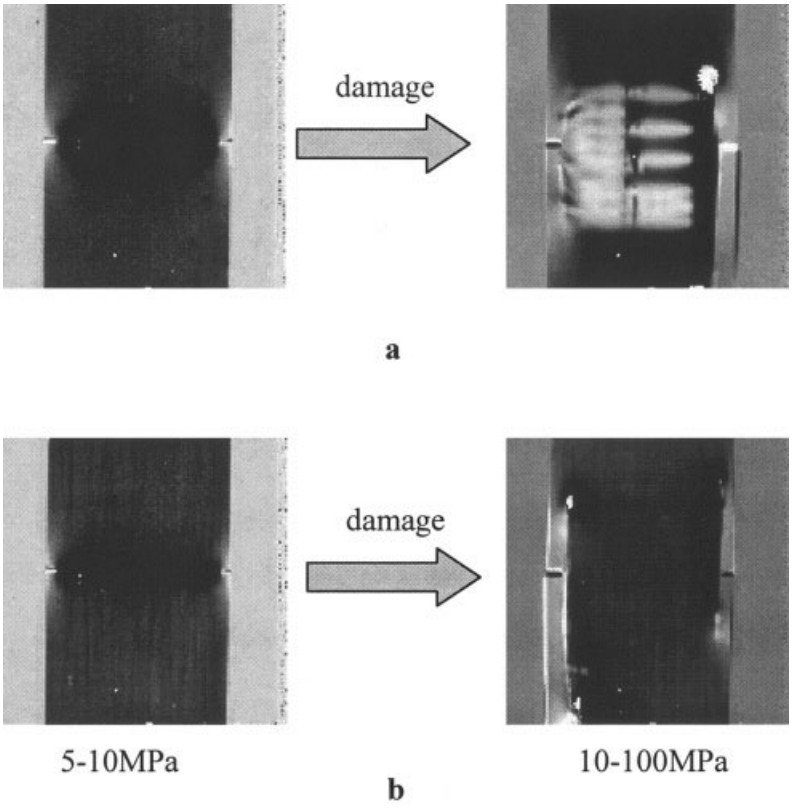

FIG. 6. The addition of a strengthening agent (6032) did not change the damage mechanism in the 636-glass/epoxy (a), while the addition of a weakening agent (6070) changed the damage mechanism to the formation of shear bands (b).

$$\Delta T = -(K \cdot T) \cdot \frac{\Delta\sigma_{kk}}{3} \tag{1}$$

where K is the thermoelastic constant.

Equation 1 relates the local temperature change to the local change in the hydrostatic stress [26–34]. A Delta Therm 1000 system was utilized to capture infrared (IR) temperature maps of each specimen during loading. The system has a maximum spatial resolution of 120 μm and a temperature resolution of 0.003° K, corresponding to a stress amplitude of roughly 1 MPa for a typical material.

TSA was performed on double-edge-notched model composite specimens to study the evolution of damage with increasing applied load. In preparation for TSA, the tabbed samples were painted with two coats of flat black paint to provide uniform surface emissivity. The composites were tested in a series of damage cycles, each with an increasing level of applied damage load, and the Delta Therm 1000 system was utilized to image the progression of damage. A detailed description of the method is described elsewhere [34].

RESULTS AND DISCUSSION

Typical stress-strain curves for 636 glass/epoxy and 646 glass/epoxy specimens with Vf $\cong$ 12% are shown in Figs. 1 and 2, respectively. Both figures show that the coupling agents had no significant effect on the mechanical properties of the composites. The as-received 646-glass/epoxy composites (no additional silanes) exhibited a small, but consistently higher elastic modulus and strength than any other sample. This difference is attributed to a slightly higher fiber volume fraction in the as-received 646-glass/epoxy (16% vs. 12%), and is not related to any differences in fiber, matrix, or interface properties. This difference is not expected to influence the results of damage evolution, because damage is found to saturate long before the composite ultimate strength is reached. Furthermore, the damage mechanism in the 646-glass/epoxy was not affected by the slightly higher volume fraction.

The first notable differences in damage evolution arise when comparing damage evolution in the untreated 636-type glass/epoxy composites with damage evolution in the untreated 646-type glass/epoxy composite (Figs. 3 and 4). The 636-type composites developed multiple matrix cracks (Fig. 3), while the 646-type composites developed shear bands (Fig. 4). The damage mechanisms in these composites are more clearly identified by utilizing a new method of damage imaging (Fig. 5) [34]. Figure 5 clearly shows the mechanism of multiple matrix cracking in the 636-type samples and shear bands in the 646-type samples.

Figure 6 shows the effect that interface surface treat-

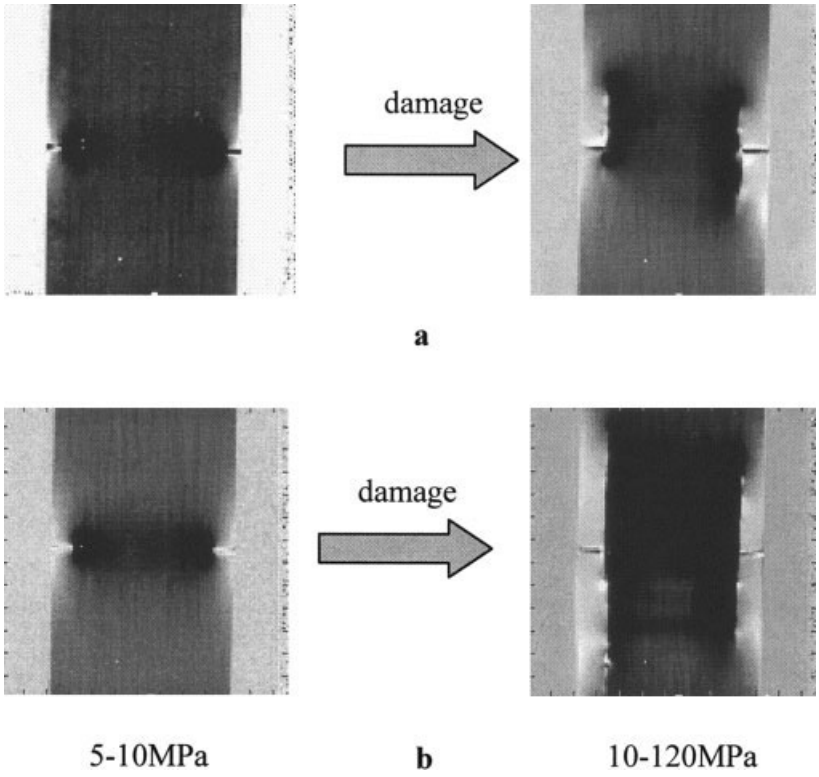

FIG. 7. The addition of surface treatments to the 646-glass/epoxy composite did not change the damage mechanism. However, the onset and absolute growth of damage was delayed by the addition of a strengthening agent (6032) (a) and enhanced by the addition of a weakening agent (6070) (b).

ments had on the ensuing damage mechanism in 636-type glass/epoxy composites. The addition of an interface-strengthening agent (Z6032) had no effect on the damage mechanism (Fig. 6a). However, the addition of an interface weakening agent (Z6070) shifted the damage mechanism from multiple matrix cracking to the development of shear bands (Fig. 6b). The shift in damage mechanism from one of multiple matrix cracking for untreated fibers and strong interfaces to one of shear banding for weak interfaces (Z6070 treated fibers) is consistent with the expected effects of the Z6070 silane additive. The Z6070 additive is expected to weaken the interface bond, making crack deflection into the interface more likely.

Figure 7 shows the effect of interface treatments on damage evolution in the 646-type glass/epoxy composite ($V_f \cong 12\%$). In each case, shear bands develop with increasing applied load. Recall that shear banding was also observed in the untreated 646-type composite. The use of the Z6032 coupling agent is expected to improve the fiber/matrix interface bond, making it more likely for multiple matrix cracking to occur. In this case, however, no shift in damage mechanism was observed with use of the Z6032 silane treatment. As such, the coupling agent that is applied to the fibers at fiber production supercedes the addition of matrix additives and dominates the resulting interface properties. No shift in damage mechanisms was anticipated with the use of the Z6070 fiber treatment because this coupling agent is designed to weaken the interface bond. A weaker interface bond facilitates the deflection of cracks into the fiber/matrix interface, making shear banding more likely. Comparing Fig. 7a and b with Fig. 4 reveals that the shear bands form at lower load and extend further from the notch plane for composites treated with the weakening agent (Z6070).

CONCLUSIONS

Model glass fiber reinforced epoxy composites were utilized to explore the effect of interface properties on damage evolution. Composites using 636-type glass fibers exhibited multiple matrix cracking, while 646-type glass fiber composites developed shear bands. The observed differences in damage evolution could be attributed to two possible causes: 1) the 646 fibers are known to be stronger than 636 fibers, and 2) the 646 fibers are produced with a silane coupling agent that is applied during fiber fabrication. Because damage was found to saturate before fiber failure, the reason for the differences in damage mechanism is attributed to the difference in fiber surface treatments.

Coupling agents were added to the epoxy resin to alter the interface properties. Composites fabricated with 646-type glass exhibited shear band formation regardless of the addition of matrix additives. This damage mechanism and the insensitivity to additives is attributed to the fiber coating that is used during production of the 646-type fibers. The 636-type glass fibers have a starch coating, while the 646-

type glass fibers have a coating composed of starch plus an added silane coupling agent. The results show that the effects of the as-processed fiber coating on the 646-type fibers supercede the effects of the coupling agents that were utilized during composite fabrication.

Addition of a weakening agent to the 636-glass/epoxy composite was found to alter the operative damage mechanism from multiple matrix cracking to shear band formation. This change in mechanism is postulated to arise from a weakening of the interface. As can be seen in Fig. 1, the change in damage mechanism was not at the expense of composite strength or ductility. As such, the damage mechanism can be altered to suit the end-use needs of the composite application without compromising the baseline mechanical properties. Similar favorable outcomes can be expected in ceramic matrix composites.

The present study shows that the damage mechanism in a composite can be altered by changing the fiber/matrix interface properties. Furthermore, these results indicate that the damage mechanism can be changed *without* affecting the tensile strength or ductility of the composite. As such, a more favorable mechanism can be processed into the composite to allow for better stress redistribution and decreased notch sensitivity. In short, there is strong evidence that the damage mechanism can be engineered to suit the particular application, making it more likely that brittle constituent composites can be utilized in structural applications.

ACKNOWLEDGMENTS

The authors would like to acknowledge Dr. Ozden Ochoa and the Air Force Office of Scientific Research for supporting this research.

REFERENCES

1. A.G. Evans, F.W. Zok, and T.J. Mackin, *High Temperature Mechanical Behavior of Ceramic Composites*, Butterworth-Heinemann, Boston, 3–84 (1995).
2. M.D. Thouless, O. Szaibero, L.S. Sigl, and A.G. Evans, *J. Am. Ceram. Soc*., **72(4)**, 525–532 (1989).
3. F.E. Heredia, S.M. Spearing, M-Y. He, T.J. Mackin, A.G. Evans, P. Mosher, and P. Brondsted, *J. Am. Ceram. Soc*., **77(11)**, 2817–2827 (1994).
4. T.J. Mackin and T.E. Purcell, *Experimental Techniques*, **20(2)**, 15–20 (1996).
5. T.J. Mackin, T.E. Purcell, M.Y. He, and A.G. Evans, *J. Am. Ceram. Soc*., **78(7)**, 1719–1728 (1995).
6. S. Mall, D.E. Bullock, and J.J. Pernot, *Composites*, **25(3)**, 237–252 (1994).
7. G. Bao and Z. Suo, *Applied Mechanics Review*, **45(8)**, 355–366 (1992).
8. Z. Suo, S. Ho, and X. Gong, *Journal of Engineering Materials and Technology*, *Transactions of the ASME*, **115(3)**, 319–326 (1993).
9. W.W. Stinchcomb and C.E. Bakis, *Fatigue of Composite Materials*, Elsevier Science Publishers B.V., New York (1990).
10. A.G. Evans, J.M. Domergue, and E. Vagaggini, *Proceedings from the Conference on Critical Issues in the Development of High Temperature Structural Materials,* TMS, Warrendale, PA, 239–278 (1993).
11. H.C. Cao, E. Bischoff, O. Sbaizero, M. Ruhle, A.G. Evans, D.B. Marshall, and J.J. Brennan, *J. Am. Ceram. Soc*., **73(6)**, 1691–1699 (1990).
12. A.G. Evans, *Materials Science and Engineering*, **A143**, 63–76 (1991).
13. R.J. Kerans, R.S. Hay, N.J. Pagano, and T.A. Parthasarathy, *Ceramic Bulletin*, **68(2)**, 429–442 (1989).
14. J. Aveston, G.A. Cooper, and A. Kelly, *Conference Proceedings, National Physical Laboratory*, JPC Science and Technology Press, 15–26 (1971).
15. W.A. Curtin, *J. Am. Ceram. Soc*., **74(11)**, 2837–2845 (1991).
16. L.T. Drzal, M.J. Rich, and P.F. Loyd, *J. Adhesion*, **16**, 1–30 (1983).
17. M.S. Madhukar and L.T. Drzal, *J. Composite Materials*, **25**, 958–991 (1991).
18. A.G. Evans, F.W. Zok, and J. Davis, *Composites Science and Technology*, **42**, 3–24 (1991).
19. T.W. Clyne and M.C. Watson, *Composites Science and Technology*, **42**, 25–55 (1991).
20. M.D. Thouless and A.G. Evans, *Acta. Metall.*, **36**, 517–522 (1988).
21. M.C. Larson, *Composites Engineering*, **5**, 25–36 (1995).
22. B. Budiansky, J.W. Hutchinson, and A.G. Evans, *J. Mech. Phys. Solids*, **34**, 167–189 (1986).
23. G. Lin, P.H. Geubelle, and N.R. Sottos, *International Journal of Solids and Structures*, **38**, 8547–8562 (2001).
24. A.K. Davis, Masters Thesis, Dept. of Theoretical and Applied Mechanics, University of Illinois at Urbana-Champaign, (1999).
25. ASTM Standard D 3039/D 3039M - 95a, *Annual Book of ASTM Standards*, ASTM International, West Conshohocken, PA (1995).
26. N. Harwood and W.M. Cummings, *Thermoelastic Stress Analysis*, Adam Hilger, IOP Publishing, New York (1991).
27. N.F. Enke, Ph.D. Thesis, The University of Wisconsin-Madison, (1989).
28. A.K. Wong, J.G. Sparrow, and S.A. Dunn, *J. Phys. Chem. Solids*, **49(4)**, 395–400 (1998).
29. A.K. Wong, R. Jones, and J.G. Sparrow, *J. Phys. Chem. Solids*, **48(8)**, 749–753 (1987).
30. B. Budiansky and R.J. O'Connell, *J. Geophysical Research*, **88(B12)**, 10343–10348 (1983).
31. B. Budiansky, *J. Comp. Materials*, **4**, 286–295 (1970).
32. M.W. Zemansky, *Heat and Thermodynamics*, 5th edition, McGraw-Hill, New York (1968).
33. E.A. Jackson, *Equilibrium Statistical Mechanics*, Prentice-Hall International Series in Engineering of the Physical Sciences, Englewood Cliffs, NJ (1968).
34. T.J. Mackin and M.C. Roberts, *J. Amer. Ceram. Soc*., **83(2)**, 337–343 (2000).